



## Modifying the Strength of Soft Soils via Heating and Cement Grouting Method



Ali H. Shareef<sup>\*</sup>, Mohammed A. Al- Neami<sup>id</sup>, Falah H. Rahil<sup>id</sup>

Civil Engineering Dept., University of Technology-Iraq, Alsina'a street, 10066 Baghdad, Iraq.

\*Corresponding author Email: [bce.20.36@grad.uotechnology.edu.iq](mailto:bce.20.36@grad.uotechnology.edu.iq)

### HIGHLIGHTS

- This study examines the effect of time on strength and degree of improvement of grouting material in heated, cracked soil.
- The shear strength of the heated soil increased from 14 to 300 kPa
- At 15% settlement ratio, bearing ratio rose from 32.9 to 71.7 as water-cement ratio increased from 0 to 1.25
- At 15% settlement, ultimate bearing capacity ratios decreased from 14.3 to 11.4 for models with 1.25 to 1.75 water-cement ratios
- At 15% settlement, bearing ratios for heating and 1.25 water-cement grouting were 71.70, 88.19 and 98 for different curing times

### ARTICLE INFO

**Handling editor:** Wasan I. Khalil

**Keywords:**

Soft soil; Bearing capacity ratio; Grouting, Heating;Portland cement; Curing period.

### ABSTRACT

Soft clayey soils present geotechnical engineering challenges with significant stability and settlement. Various methods are employed to enhance the geotechnical properties of these soils. Heating and grouting are the methods used to improve such soil. A new heating and cement grouting system using gas as a source of heating through boreholes and Portland cement for grouting was designed and manufactured to enhance the soft soil. Different parameters were investigated, including the shear strength and the angle of internal friction, as well as the water/cement ratio, W/C (0.5, 0.75, 1, 1.25, 1.5, and 1.75), and the period of curing (3, 14, and 28 days). The results showed the shear strength and angle of internal friction increased from 14 to 300 kPa and 0 to 50 degrees, respectively. If only the heating system is running, the strength and behavior of the soil will improve via heated and cement grouting with a water/cement ratio. If the w/c ratio increases from 0 to 1.25, the ultimate bearing capacity ratio ( $q_u$  treated/ $q_u$  untreated) increases from 6.5 to 14.3 at 15% settlement. However, when the water/cement ratio increases from 1.25 to 1.75, the ultimate bearing capacity ratio ( $q_u$  treated/ $q_u$  untreated) decreases from 14.3 to 11.4. The ultimate bearing capacity ratio improves with increasing curative time. It climbs from 14.3 to 19.6 during 3 to 28 days for cement grouting models, while the ultimate bearing capacity ratio grows from 6.5 to 7 during 3 to 28 days for heating process models only, at 15% settlement.

## 1. Introduction

Buildings erected on soft soils may fail owing to their low strength, and excessive settling of the soil under an exterior load might occur, so improvements for soft soils must be made before construction to minimize or decrease the maintenance cost or failure of buildings [1]. The building of tunnels, mining operations, and hydroelectric engineering projects may often encounter collapses, instability, and the influx of clay and water [2]. These issues are typically attributed to soil with inadequate strength or permeability. Thermal treatment is the process used to strengthen and improve the behavior of unstable soils. In recent years, numerous studies on the impact of elevated temperatures on soil quality have been published. Heat treatment decreased the soil's liquid and plastic limits, optimal water content, unconfined compressive strength, and expansion pressure after being examined in the laboratory for its influence on three varieties of clay from northern Jordan [3]. Any land-based construction needs a solid foundation to sustain the entire structure, which is why it is so crucial. The soil beneath the foundation is extremely important for its strength. Some projects require the use of additives or reinforcements because the soil compacted by modifying energy is inadequate to produce the desired effects [4]. Grouting reinforcement is a valuable strategy for enhancing soil characteristics, particularly in terms of augmenting strength and durability and mitigating permeability [5-7]. The process involves the injection of grout slurry into the soil; different grout slurries are used for grout reinforcement. The selection of a specific grout slurry for a particular project is contingent upon the intended purpose of grouting and the soil characteristics involved. The variety of slurries used may vary from cement-based grout slurries, such as cement slurry and

cement-sodium silicate slurry, to chemical slurries, such as lignin, acrylic, urea, or epoxy resins [8]. Despite possessing changeable gel time, excellent penetration, and flexibility after solidification, chemical grout is limited in its uses because of its high cost, lesser solid strength, and reduced durability [9]. Moreover, they have the potential to do damage to the surrounding environment. Cement and cement-sodium silicate slurries are widely used as grout slurries in soil grouting projects owing to their cost-effectiveness, abundant availability of raw materials, superior solid strength, commendable endurance, and compatibility with the surrounding environment [10].

The rheological properties of cement slurry and cement-sodium silicate slurry exhibit significant disparities. The change in viscosity of cement slurry over the grouting period is not significant enough to visibly impact other parameters, such as grouting pressure and grout slurry space distribution. Therefore, the viscosity of cement slurry was believed to remain constant over time [11]. It is supposed that the viscosity of the cement slurry remains constant during the grouting operation. Nevertheless, it is worth noting that the viscosity of a cement-sodium silicate slurry experiences a rapid rise over time and may be effectively regulated by manipulating the various components involved [11]. The viscosity of the material, which varies with time, has a notable impact on several parameters, including grouting pressure and the dispersion of grout slurry [12]. The rheological behavior of cement-sodium silicate slurry was investigated by [13], who examined various volume ratios between the cement slurry and water glass.

Based on the obtained findings, the author posited a conceptual framework whereby the cement-sodium silicate slurry setting process may be delineated into three distinct phases: the initial low-viscosity stage, the subsequent stage of viscosity augmentation, and the final stage of solidification. In the initial combination, there is a gradual and minimal rise in viscosity. However, this is followed by a rapid increase in the viscosity and a subsequent drop in fluidity. Eventually, the cement-sodium silicate slurry solidifies and progressively loses its fluidity. Applying uniaxial compression to grouted cylindrical specimens is a commonly conducted test in soil research. This test aims to investigate the impact of various grouting parameters, such as soil composition, grout slurry, and grouting pressure, on the effectiveness of soil grouting. In a study by [9], uniaxial and biaxial compressive tests were performed on specimens injected with cement slurry or modified cement slurry containing urea formaldehyde resin as an additive. [14] designed and implemented a grouting simulation test apparatus to investigate the formation and progression of grout balls and cracks inside clay using cement slurry. The findings of their study suggest that the process of fracture grouting in clay may be categorized into three distinct stages: the grout ball stage, the first fracture surface stage, and the subsequent fracture surface stage. It was observed that each fracture takes place along the weakest surface. The study of [13] developed a comprehensive experimental apparatus to replicate the phenomenon of grout splitting inside fault fracture zones. They pointed out that the process of grouting and splitting in the soil can be categorized into three distinct phases: energy buildup, soil fracturing, and slurry energy transfer. These stages are identified by analyzing the grouting pressure versus time curves and considering energy dissipation. [15] used a custom-designed in-situ grouting experimental apparatus to examine the underlying processes and progression of slurry fracturing using bentonite slurry.

The experiments demonstrate the phenomenon of slurry fracture and extension. A significant portion of the soil in the center and south of Iraq is weak clay. The construction of projects on these soils presents a challenge; consequently, it is necessary to enhance these soils, notably in these regions, which require promoting economic and development projects in various disciplines. Therefore, the technique used to enhance this soil must be cost-effective, rapid implementation, and permanent. Iraq is regarded as an oil-rich nation with an abundance of wells and oil refineries. Also, Iraq is considered a cement-producing nation, so fissures caused by heating should be filled with heat-resistant cement. Implementing the heating method with cement grouting in such areas is successful and cost-effective due to these factors. Therefore, this study aims to enhance the resistive strength of soft clay soils treated with heating by using cement grouting with different cement-to-water ratios to treat cracks resulting from the heating process. The effect of time on the strength and degree of improvement of grouting material in cracks in soil exposed to heat will also be studied.

## 2. Experimental Work

### 2.1 Material Used

Four materials are used in this study: Soil, gas, water, and Portland cement. The specifications of each material are as follows: The soil sample used in this study was brought from the Al-Amer site in Baghdad city. The physical and chemical properties of the soil used are listed in Table 1, and the grain size distribution of the soil used is plotted in Figure 1. Cooking gas and tap water are used in this study. The cement used is sulfate-resistant Portland cement (type V). Table 2 shows the physical and chemical properties of the cement. The tests were conducted in the Central Laboratory Department of the Iraqi Geological Survey.

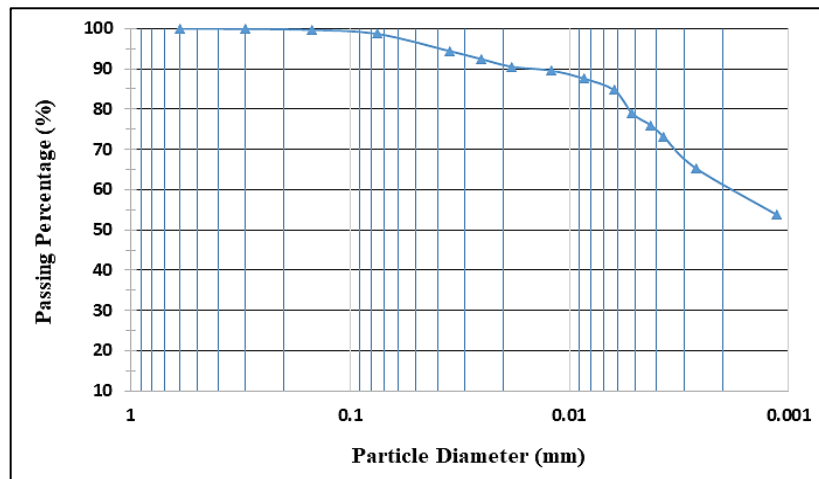


Figure 1: Particle Size Distribution of Soil Used

Table 1: Physical and Chemical Properties of Natural Soils Used

Index Property	Test Standard	Index Value Soil A
Initial water content(%)		10
Liquid Limit (L.L.)(%)	ASTM D4318	44
Plastic Limit (P.L.)(%)	ASTM D4318	23
Shrinkage Limit (S.L.)(%)	ASTM D427	19
Plasticity Index (P.I.)(%)	ASTM D318	21
Specific Gravity (Gs)	ASTM D854	2.69
Gravel (larger than 4.75 mm) (G)%	ASTM D422	0
Sand (0.075 to 4.75 mm) (S)%	ASTM D422	2
Silt (0.005 to 0.075 mm) (M)%	ASTM D422	20
Clay (less than 0.005 mm) (C)%	ASTM D422	78
Classification (USCS)	ASTM D2487	CL
Organic Matter (O.M.)(%)	ASTM D2974	< 0.01
Total Dissolved Salt (TDS%)	ASTM D5907	2.21
Total Solved Salt (TSS%)	ASTM D5907	8.3
pH Value(%)	ASTM D4972	7.2

Table 2: The physical and chemical properties of the Cement

Index Property	Index Value
<b>Physical Properties</b>	
Specific gravity (G.s)	3.15
Compressive strength after three days (MPa)	17
Compressive strength after seven days (MPa)	26
Time of initial setting (minute)	93
Time of final setting (hour)	4.28
<b>Chemical Properties</b>	
C <sub>3</sub> S%	57
C <sub>3</sub> A%	3.27
C <sub>2</sub> S%	29
SiO <sub>2</sub> %	19.79
CaO%	63.8
MgO%	3.19
SO <sub>3</sub> %	2.15
L.O.I%	0.89

## 2.2 The Devices and Tests Used in This Study

To explore the response of heated soft clay soil and cement grouting, it is important to simulate circumstances similar to those that may be encountered in the field. A specific testing apparatus and its attachments are created and constructed to accomplish this objective. The devices can provide heating and cement grouting, and then a monotonic load is applied to the 200 mm by the prototype foundation. The evaluation system includes the following components: metal load framework, metal box, casing (barrier tube), heating system, and grouting system. The metal load framework is a metal structure that was created to sustain the verticality of the piston mechanism utilized to deliver the center-focused load on treated soil inside a metal box with the interior dimensions (92.5×92.5×92.5) cm<sup>3</sup> and bearing the penetration motor of the borehole casing through the heating process would be done, as shown in Plate 1.

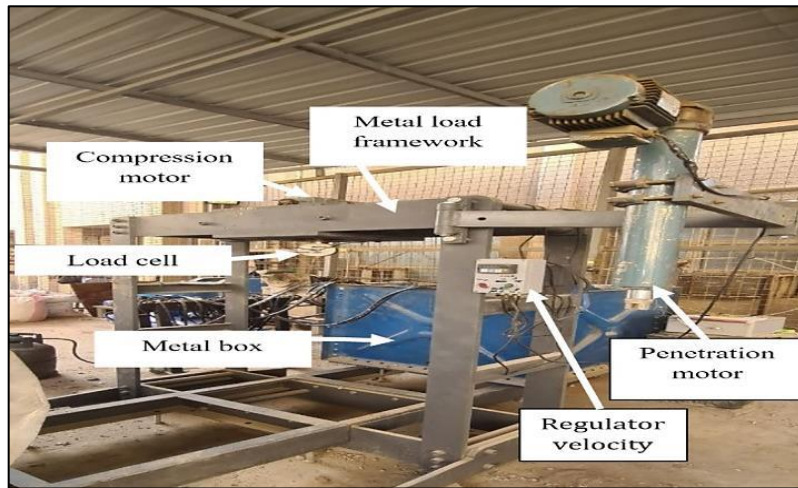


Plate 1: Metal load framework

As casing for the borehole, carbon steel casing was manufactured according to A53 ASTM grade B with an inner diameter of 35 mm and an outer diameter of 43 mm (4 mm thickness) with a 40 cm depth. The heating system was fabricated and installed to create heat inside the soil model. The system is composed of five major components: First, combustion pipes. Second, rubber pipelines (W/BP 20/30 BAR) transmit gas and air from the source to the priming pipes. Thirdly, the control of the heating source. Fourthly, an air compressor to provide the heating system with air. Also, the gas bottle and gas regulator. Lastly, measuring devices measure the heating system, as seen on Plate 2 (A, B, C, and D).

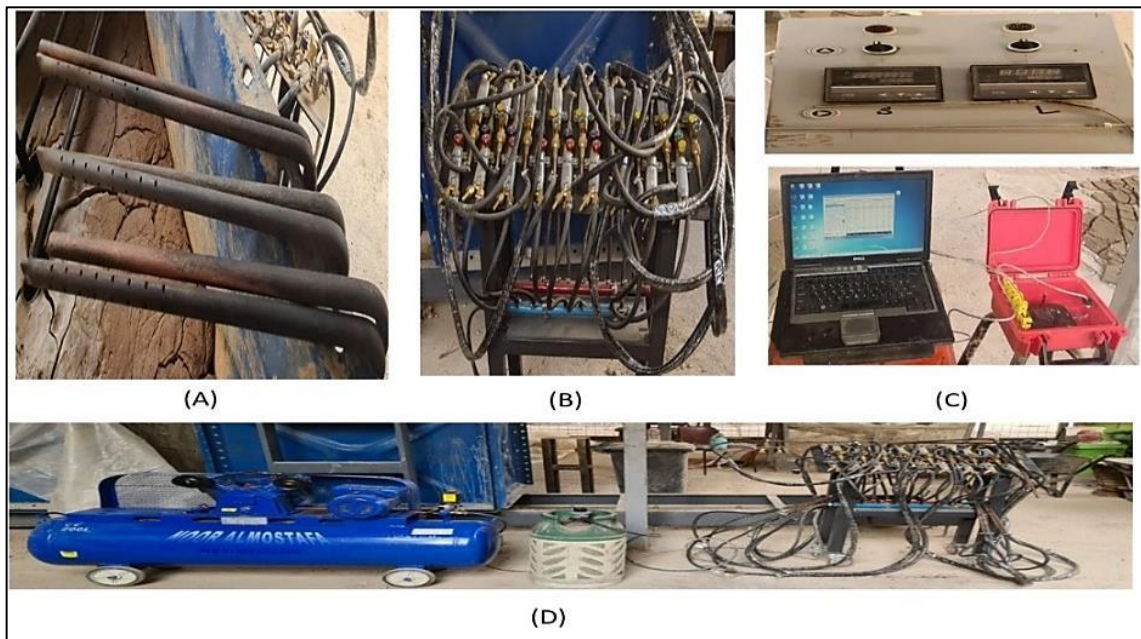
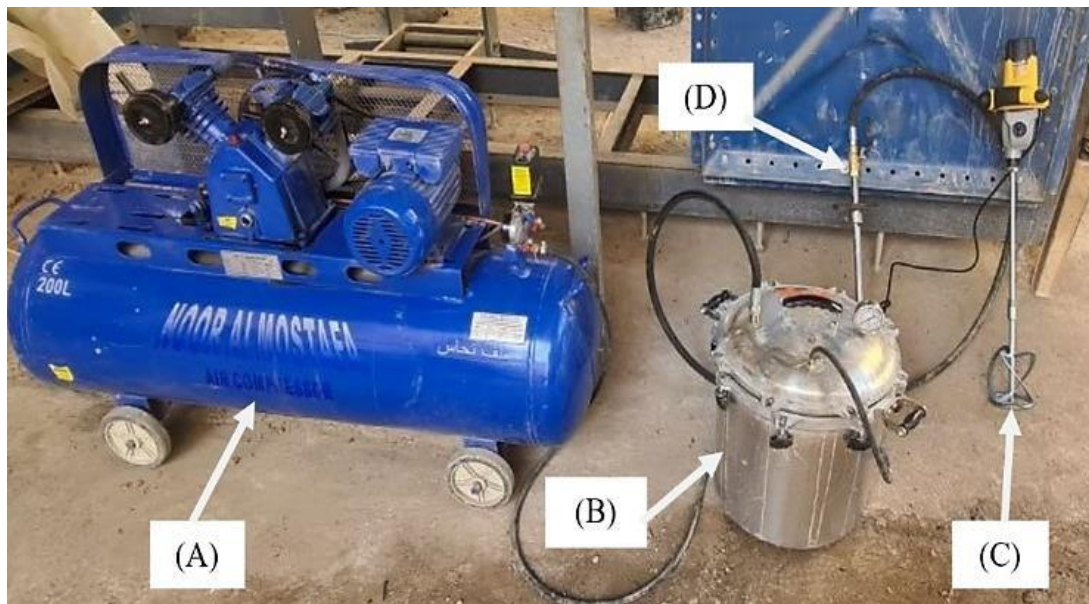


Plate 2: The System of Heating ((A) combustion pipes, (B) the control of the heating source, (C) measuring devices in the heating system, and (D) air compressor, the gas bottle, and gas regulator

The grouting system depicted in Plate 3 has been devised and constructed specifically for this study. The equipment comprises four primary components: The modified autoclave with a pressure tolerance of 2 bars. Secondly, an air compressor is needed to provide the grouting system with air pressure. Thirdly, the grouting mixer is a device used for mixing grout materials. The grouting material has been blended using a consistent-speed drill, operating within the range of 60 to 300 revolutions per minute. The mixer is equipped with a wing to facilitate the mixing process. Lastly, the open-end tube for cement grouting has a 25 mm diameter and 60 cm length. This tube contains a cap with a 35 mm inner diameter and a 50 mm outer diameter to prevent the material grouted from escaping outside the borehole; it also includes a valve to make the grouting process easy and accurate, as shown in Plate 4.





**Plate 3:** The system of cement grouting ((A) the Air compressor, (B) The modified autoclave, (C) The grouting mixer, and (D) The tube for cement grouting



**Plate 4:** The tube for cement grouting

### 2.3 The CPT Probe Device

To measure the shear strength and the angle of internal friction values for heated treated soils (the effect of overburden pressure due to the short penetration depth has been neglected), an electrical cone penetration probe (CPT) with a cross-sectional area of  $1000 \text{ mm}^2$  is used in this investigation per ASTM D 5778. This probe is connected to the penetrating motor through a standard adapter made in Turkey, as shown in Plate 5. The penetration rate of  $10 \text{ mm/sec}$  is constant because the penetration depth is small. Also, it does not contain a water pressure sensor because of the cost of this sensor.



**Plate 5:** Prepare the CPT probe to model the test

### 2.1 Establishing the Soil Modeling and Testing Procedure

A portable vane shear device has been used to determine the undrained shear strength of a clay soil sample. The obtained result indicated a shear strength value of  $14 \text{ kPa}$ , while the clay soil had  $29 \%$  water content per  $25 \text{ kg}$  of dry soil. A laboratory mixer with a capacity of  $120 \text{ liters}$  was used for blending purposes. The soil was enclosed inside polythene bags for one day after mixing to achieve consistent moisture content. Subsequently, the dirt was placed in a metal container measuring  $92.5 \text{ cm} \times 92.5 \text{ cm} \times 92.5 \text{ cm}$ , with each layer being put at a depth of  $10 \text{ cm}$ . A  $60 \text{ mm} \times 60 \text{ mm}$  wooden ram was used to gently compact the soil to get rid of any trapped air. Following the application of the final layer, the upper surface undergoes a cleaning and leveling process. Subsequently, a hardwood platform, possessing an equivalent surface area to the bed's soil, is positioned onto the bed. This platform is subjected to a sitting pressure of  $5 \text{ kPa}$  for one day. Upon alleviating the seat pressure, proceed to position the guide plate according to the distinct arrangement, spacing, and length of the nine boreholes for the

cases. This will facilitate the successful installation of the said cases. Subsequently, employ a motor with a regulated velocity to penetrate the cases. Following this, employ a 34.5 cm-diameter auger to excavate and remove the soil contents within the aforementioned cases. After this procedure, the guide plate and motor must be removed, allowing the soil model to be prepared for the heating process. The initiation of the heating phase in borehole scenarios is facilitated by combustion hands, which are heating pipes. Once the casing is inserted into the soil and the gas and air ratio is adjusted to 10% gas and 90% air, the heating system is triggered, and the heat transfer starts from the casing to the soil. The ignition of the casing fire is facilitated by pipe primers. The parameters constant throughout this study for the borehole heating system were a  $3D$  ( $\cong 13$  cm) separation between boreholes, a heating duration of eight hours, a casing depth of 40 cm, and a square pattern configuration. Following the completion of the procedure, the heating equipment is deactivated, thereby allowing the soil model to undergo a cooling process for 24 hours until it reaches the surrounding ambient temperature. During the grouting operation, it is necessary to adhere to the following stages to prepare the slurry cement: Firstly, the extraction of borehole cases is achieved using a penetration or removal motor. Secondly, considering the necessary quantity of cement for resistance and the varying proportions of water with varied water-cement ratios (W/C) (0.5, 0.75, 1, 1.25, 1.5, and 1.75), the cement should be added to a mixture of water, with or without the inclusion of a plasticizer. This mixture should then be placed in a container inside a modified autoclave. Subsequently, the components should be thoroughly mixed using a mixer for about three minutes. Additionally, after combining the water-to-cement ratio using a mixer, proceed to securely seal the modified autoclave apparatus. Subsequently, carefully introduce the cement grouting tube into the designated heating borehole. In the fourth step, an air compressor produces a pressure of 2 bar inside a modified autoclave apparatus. This pressure is utilized to eject cement grout at the aforementioned pressure. Subsequently, the cement grouting tube valve is opened to facilitate filling heated boreholes.

Finally, after the grouting operation has been completed, it is essential to thoroughly clean the equipment to avoid any potential harm from solidifying the grouting material. Following the completion of the test model preparation, the 20 cm x 20 cm footing was positioned in the center of the dirt surface. The metal box was repositioned to line the centers of the footing and pressurize the motor at a 1 mm/min loading rate. Subsequently, the loading transducer and linear variable differential transformer (LVDT) were fitted. Failure can be defined as the point at which the applied load leads to a settlement equivalent to 10% of the width of the footing. However, it is important to note that vaporized water escaping from the upper layer can result in significant cracks forming in this layer. In such cases, a settlement depth of 2 cm, corresponding to 10% of the footing width, may not be a reliable criterion for assessing the state's weakness. In this study, all models consider a settlement equivalent to 15% of the width of the footing resulting from the failure load. Plate 6 (A-H) illustrates the sequential procedures involved in preparing the soil module, including heating and cement grouting treatment, culminating in the load test.

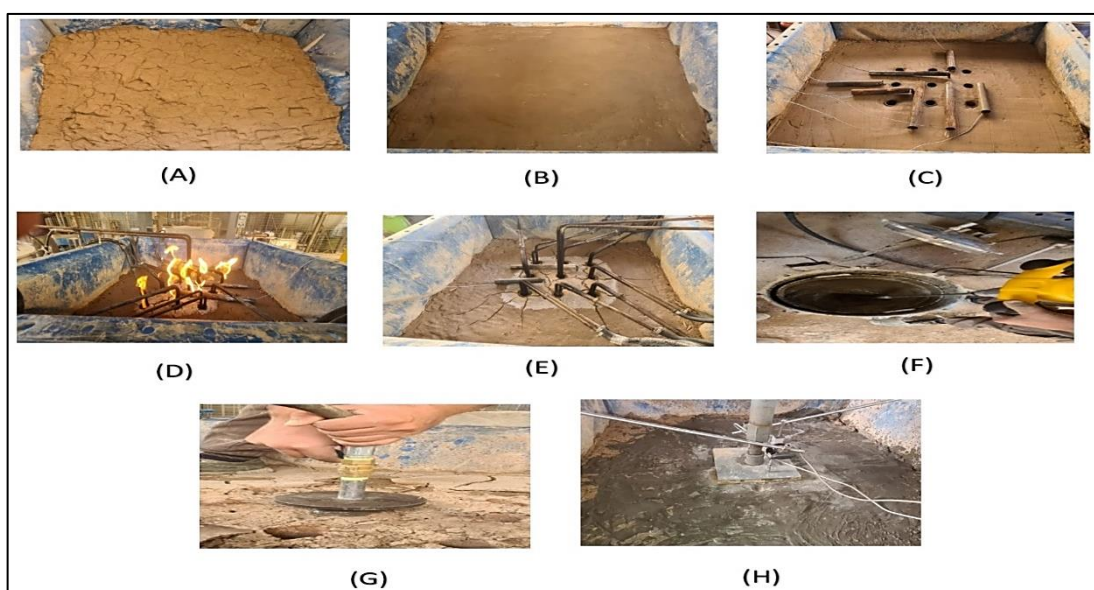


**Plate 6:** The stages of the test procedure of soil improvement by heating and cement grouting for load test ((A) Place the soil inside the box, (B) Reaching the required level, (C) Heat system implantation, (D) Operating the heat system, (E) Complete the burning process, (F) Mixing cement and water inside the injection system, (G) Cement injection into the soil improved by heat, (H) The load test

### 3. Presentation and Discussion of Test Results

#### 3.1 The Impact of Heating Treatments

To investigate the impact of heating on bearing capacity, three models were created via the square pattern with nine casing boreholes of 3.5 cm in inner diameter and 40 cm in depth. The model was heated for 8 hours. The distance spacing and the extended depth of the borehole casing were  $3D$  and 40 cm (2b), respectively. Figure 2 depicts the dimensionless relationship between the bearing ratio ( $q_u/C_u$ ) and the settlement ratio ( $Settl./b_{footing}$ ) for all models (untreated soil and without casing, untreated soil and with a casing, and treated soil after 8 hours of heating). The values of the bearing ratio ( $q_u/C_u$ ) increase at 15% of the settlement ratio ( $Settl./b_{footing}$ ) from 5.03 to 31.19, where the bearing capacity increases with the heating operation

because the bearing capacity parameters increase. Figure 3 (a and b) illustrates the variation of shear strength and angle of internal friction with depth using the CPT device. Where the shear strength increases from 14 kPa to 300 kPa (as average), the angle of internal friction drops from 0 to 50 degrees (as average), as shown in Plate 7.

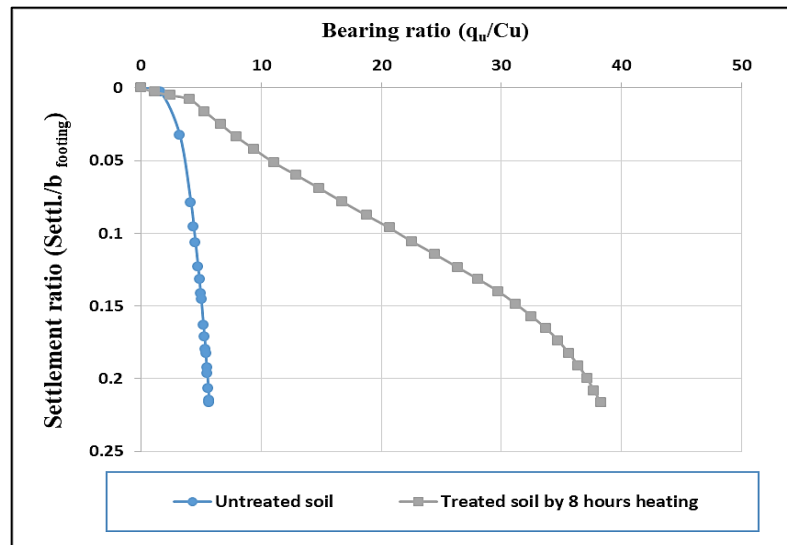


Figure 2: The dimensionless connection between the bearing ratio and the settlement ratio for treated and untreated soils by heating

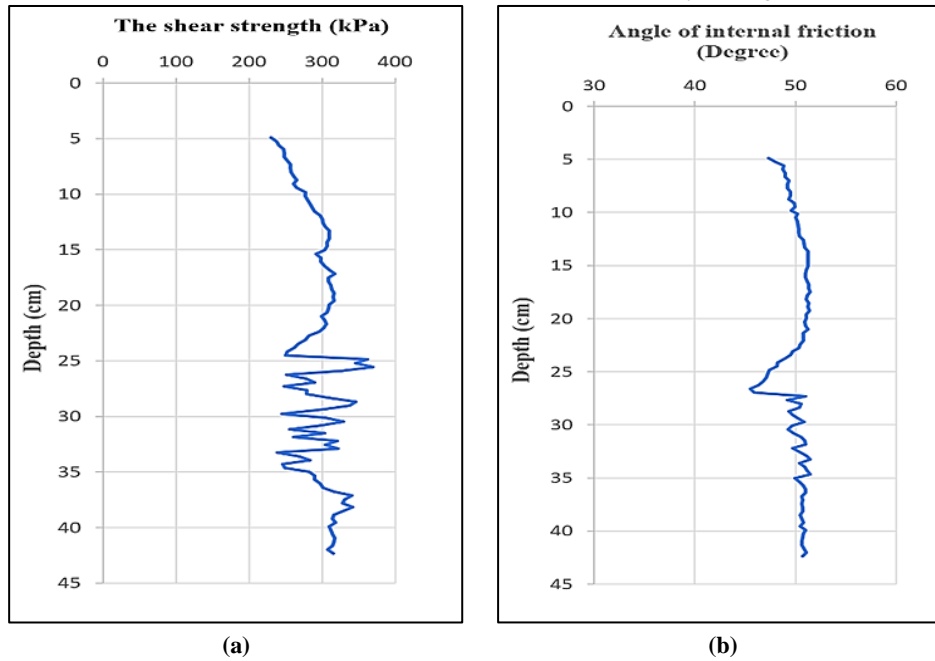


Figure 3: The variation of shear strength and angle of internal friction with depth



Plate 7: The end test of CPT probe depth



### 3.2 The Impact of The Different Water-Cement Ratio

Seven models were carried out to investigate the effect of various water-cement ratios on bearing capacity. Six models were executed with different water-to-cement ratios (0.5, 0.75, 1, 1.25, 1.5, and 1.75) for cement grouting, and one model was executed without cement grouting and tested 3 days after cement grouting or without grouting. Figure 4 illustrates the dimensionless relationship between the bearing ratio ( $q_u/C_u$ ) and the settlement ratio ( $Settl./b_{footing}$ ) without grouting at 0.5, 0.75, 1, 1.25, 1.5, and 1.75 water/cement ratios of cement grouting, respectively. The use of grouting increases the bearing ratio ( $q_u/C_u$ ). At a 15% settlement ratio, the values of the bearing ratio ( $q_u/C_u$ ) for the without grouting, 0.5, 0.75, 1, 1.25, 1.5, and 1.75 water/cement ratio of cement grouting are 32.9, 41.9, 50.5, 59.9, 71.7, 62.6, and 57.4, respectively. The boost in efficiency is because the slurry functions as a cementation material that occupies the location of heating cases when taken out at the end of the heating process,

produces treated soils with a cohesion stronger than that of heated-treated soils only, as shown in Plate 8. Also, the slurry's pressure may affect the part's orientation, which increases friction.

Figure 5 shows the ultimate bearing capacity ratio ( $q_{u \text{ treated}}/q_{u \text{ untreated}}$ ) with different percentages of the water/cement ratio of cement grouting without grouting: 0.5, 0.75, 1, 1.25, 1.5, and 1.75 models, respectively. From this figure, if the water-cement ratio increases from 0 to 1.25, the value of the ultimate bearing capacity ratio ( $q_{u \text{ treated}}/q_{u \text{ untreated}}$ ) increases from 6.5 to 14.3. However, when the water-cement ratio increases from 1.25 to 1.75, the ultimate bearing capacity ratio ( $q_{u \text{ treated}}/q_{u \text{ untreated}}$ ) decreases from 14.3 to 11.4. The highest value of the ultimate bearing ratio is achieved when the water-to-cement ratio is 1.25, equal to 71.7, because the ratio of water to cement has the greatest impact on the rheology of cement grout. When  $W/C = 0.5$ , the flow pattern of grout is power-law fluid; when  $W/C$  is from 0.7 to 1, the flow pattern is Bingham fluid; and when  $W/C$  is greater than 1, the flow pattern of grout is Newtonian [13]. Where  $W/C$  equals 1.25 with grouted pressure, the cementation material reaches as far as possible in the heated, treated soil and fills all cracks and voids. Also, as shown in Figure 3, when the water-to-cement ratio is greater than 1.25, the ultimate bearing capacity ratio ( $q_{u \text{ treated}}/q_{u \text{ untreated}}$ ) decreases because the strength of cement grouting materials decreases when a small amount of cement is combined with a large amount of water, thereby reducing the strength of cementation material within cement grouting inside the cracks and voids.

When using a water-to-cement ratio of 0.5, the quantity of cement is ten kilograms, and the prevalence of injection materials is low, as shown in the plate 9. Using a water-to-cement ratio of 1.25, the quantity of cement is 25 kilograms. This indicates that when the water-cement ratio is 1.25, all cracks and voids caused by the heating process are filled with the maximum grout pressure of 2 bar; if the grout pressure exceeds 2 bar, heaving happens in the treated soil and leads to the failure of heated treated soil models. Table 3 includes the ultimate bearing capacity ratio values given by the impact of the different water-cement ratios for cement grouting models.

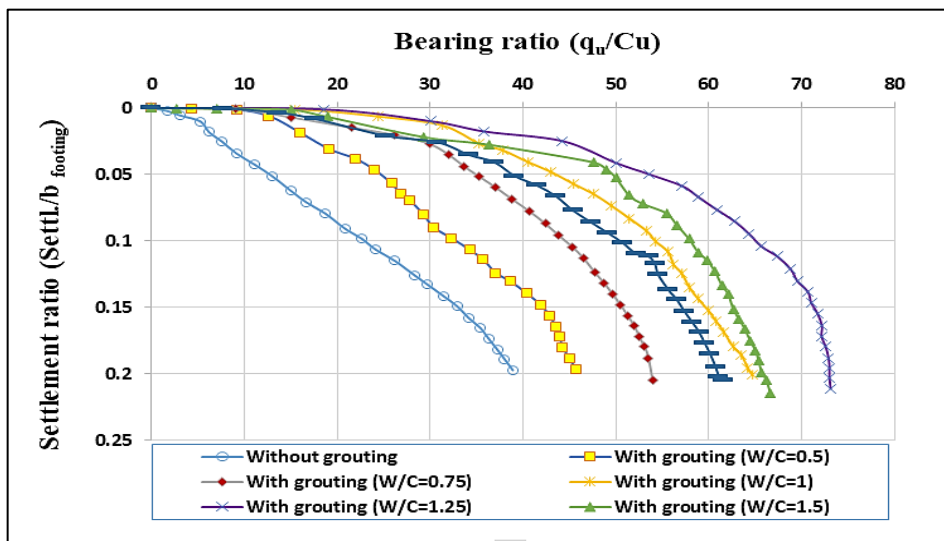


Figure 4: The dimensionless connection between the bearing ratio and the settlement ratio for various water-cement ratios of cement grouting models



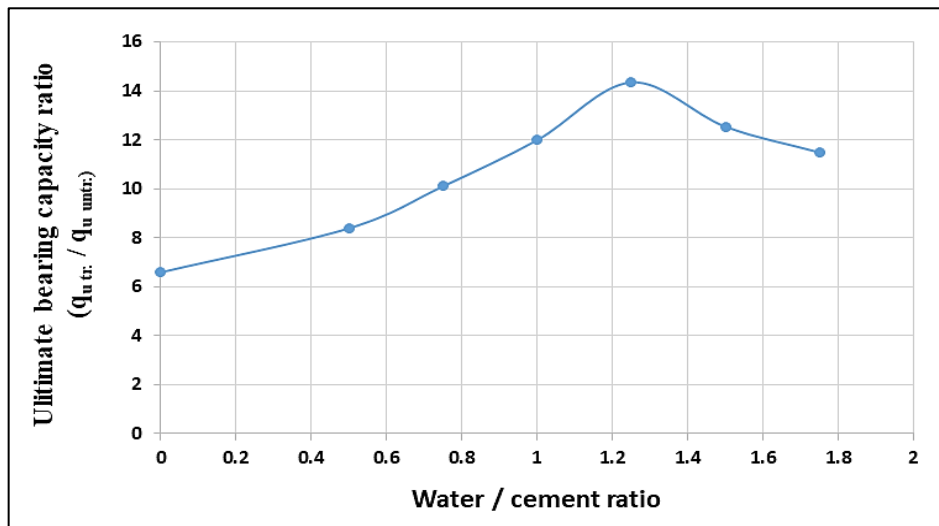


Figure 5: The dimensionless relationship between the ultimate bearing capacity ratio and the water-cement ratio of cement grouting models



Plate 8: The heated treated soil with cement grouting content of 1.25 of water cement ratio



Plate 9: The heated treated soil with cement grouting content 0.5 of water cement ratio

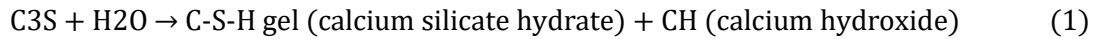
Table 3: The ultimate bearing capacity ratio values at the various water-cement ratios of cement grouting

The experimental variable	The percentage of water-cement ratio (W/C)	The ultimate bearing capacity ratio
<i>The water-cement ratio (W/C)</i>	0	6.5
	0.5	8.3
	0.75	10.1
	1	11.9
	1.25	14.3
	1.5	12.5
	1.75	11.4

### 3.3 The Impact of The Curing Period of Cement Grouting

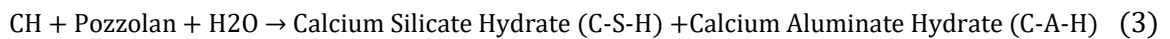
The curing period is one of the most important aspects of the study of cement grouting because the strength of cementation materials increases with time, which is related to the cement's hydration and pozzolanic reactions, particularly for cement. Cement hydration and pozzolanic reactions are two fundamental procedures in construction and cementitious materials.

Hydration of cement refers to the chemical reaction that takes place between cement and water, culminating in the formation of cement paste. Calcium silicates, such as tricalcium silicate ( $C_3S$ ) and dicalcium silicate ( $C_2S$ ), are the primary constituents of cement. Upon adding water to cement, the following reactions occur:



The C-S-H gel is responsible for the strength and durability of the cementitious material. In contrast, calcium hydroxide (CH) contributes some additional strength but is less preferable regarding long-term performance. Hydration is exothermic, meaning it releases heat, which is why curing concrete can become heated. Controlling the curing process is necessary to guarantee proper hydration and the development of desirable properties in the hardened cement paste.

In the presence of water, a pozzolan material reacts with calcium hydroxide (CH) to produce the pozzolanic reaction. Pozzolans are substances used to enhance the properties and efficacy of cement. The most common pozzolans are fly ash, silica fume, and slag. The following represents the reaction:



Pozzolans react with the byproduct of cement hydration, calcium hydroxide, to produce additional calcium silicate hydrate (C-S-H) and calcium aluminate hydrate (C-A-H). This reaction contributes to the cementitious material's overall strength and durability, enhancing its resistance to chemical attack and reducing shrinkage. The pozzolanic reaction is a slower process than cement hydration, and it can persist for an extended time, thereby contributing to the cementitious material's long-term performance. Both cement hydration and pozzolanic reactions play significant roles in forming strength, durability, and other properties of cementitious materials, such as concrete or materials grouted inside soils or rocks.

To investigate the effect of the curing period of cement grouting on bearing capacity, one should know the increase in bearing capacity for treated soils by heating processes with different periods, such as the curing period of cement grouting in models. For this purpose, four models were constructed without cement grouting and tested for various durations (1, 3, 14, and 28 days). Figure 6 illustrates the dimensionless relationship between the bearing ratio ( $q_u/c_u$ ) and the settlement ratio ( $\text{Settl.}/b_{\text{footing}}$ ) for (1, 3, 14, and 28) days of the heating process only for models, respectively. The bearing ratio increases with time ( $q_u/c_u$ ). At a 15% settlement ratio, the values of the bearing ratio ( $q_u/c_u$ ) for the 1, 3, 14, and 28 days of the heating process are 31.19, 32.9, 34.6, and 35.2%, respectively.

To explore the effect of the curing period of cement grouting on bearing capacity, three models were executed with the same water-to-cement ratio ( $W/C = 1.25$ ) for cement grouting and tested at three, fourteen, and twenty-eight days after cement grouting. Figure 5 illustrates the dimensionless relationship between the bearing ratio ( $q_u/C_u$ ) and the settlement ratio ( $\text{Settl.}/b_{\text{footing}}$ ) for (3, 14, and 28) days of the heating process with cement grouting at a water-cement ratio equal to 1.25 of models, respectively. At a settlement ratio of 15%, the values of the bearing ratio ( $q_u/C_u$ ) for the 3, 14, and 28 days of the heating processes with cement grouting at a water-cement ratio of 1.25 have emerged as 71.70, 88.19, and 98, respectively. Figure 7 illustrates the values of the ultimate bearing capacity ratio ( $q_{u \text{ treated}}/q_{u \text{ untreated}}$ ) for the heating procedure with cement grouting over varying time intervals. In Figure 8, the ratio of ultimate bearing capacity ( $q_{u \text{ treated}}/q_{u \text{ untreated}}$ ) improves with increasing curative time. The values of the ultimate bearing capacity ratio climb from 14.3 to 19.6 during 3 to 28 days for cement grouting models, while the ultimate bearing capacity ratio grows from 6.5 to 7 during 3 to 28 days for heating process models only. As can be seen in the figures, the force grows with time. There are two possible explanations for this increase: The first is that the injected cement materials solidify within the cracks and cavities caused by the heating process, and their strength grows with time due to the outcomes of interactions between cement and water.

The second reason is that wet, cohesive soils have the sensitivity and thixotropy that clay has. Saturated clays may have lost strength because their original deposit structure has deteriorated. On the other hand, thixotropy is characterized by a softening of material upon remolding, followed by a progressive recovery to its former strength upon resting in the original shape. This is an isothermal, reversible, time-dependent process under constant composition and volume [16]. Lastly, Table 4 contains the ultimate bearing capacity ratio values determined by the heating procedure's consequences with or without cement grouting at variable time intervals.

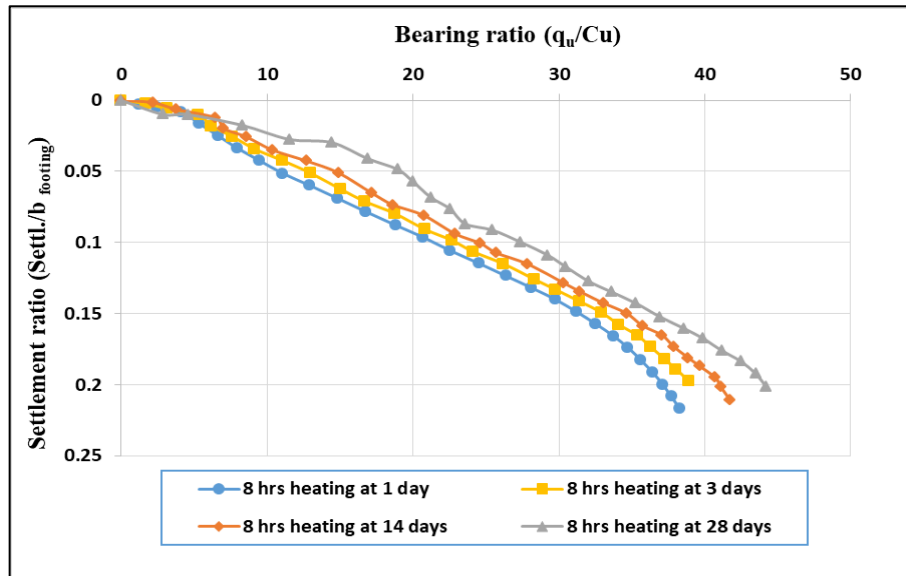


Figure 6: The connection dimensionless between the bearing ratio and the settlement ratio for various curing periods of the heating process only

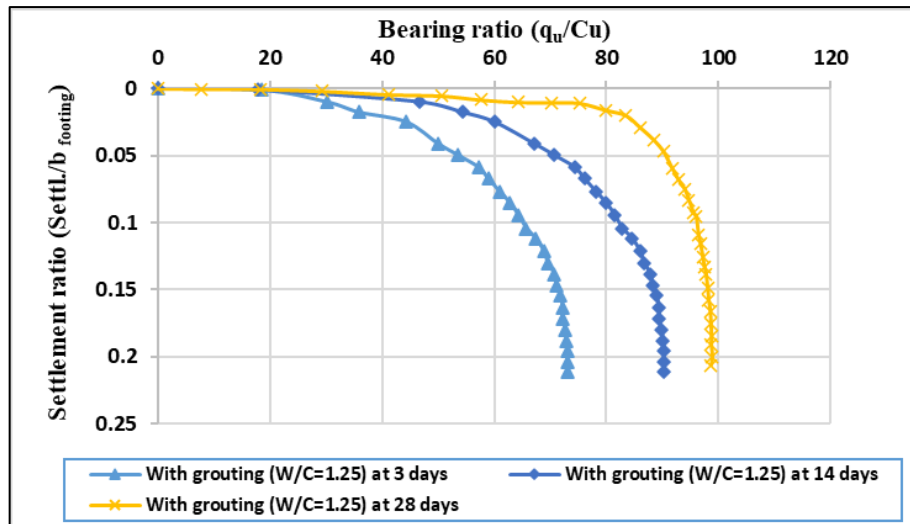


Figure 7: The connection dimensionless between the bearing and settlement ratios for various curing periods of the heating process with cement grouting

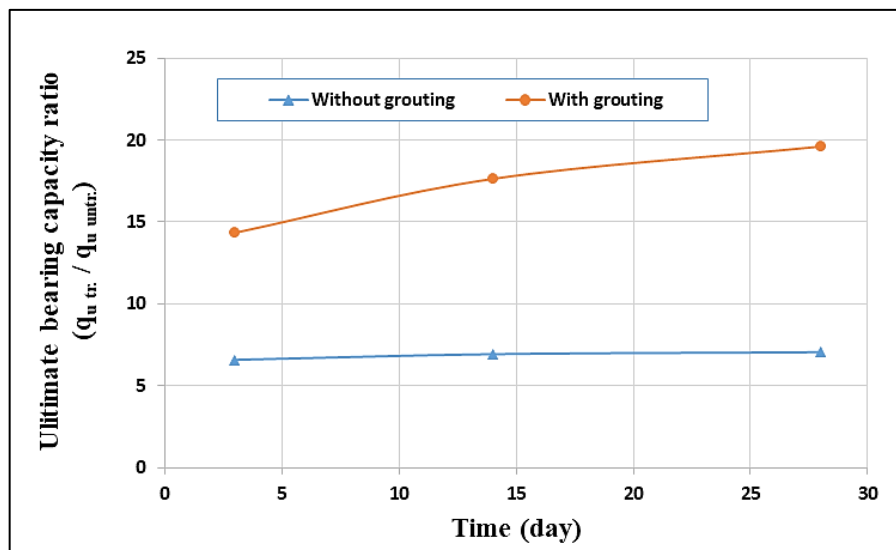


Figure 8: The relationship between the ultimate bearing capacity ratio and the curing period for the heating process with or without cement grouting



**Table 4:** The ultimate bearing capacity ratio values at the various curing periods of the heating process with or without cement grouting (W/C=1.25)

The experimental variable	The curing time (day)	The ultimate bearing capacity ratio	
		Without grouting	With grouting
<i>The curing period</i>	1	6.23	---
	3	6.5	14.3
	14	6.92	17.63
	28	7	19.6

#### 4. Conclusion

Based on the findings of the present investigation, the following deductions may be drawn:

- When the heating system was running, the shear strength and angle of internal friction increased from 14 to 300 kPa and 0 to 50 degrees, respectively.
- The bearing ratio increases from 32.9 to 71.7 at a 15% settlement ratio if the water-to-cement ratio (W/C) increases from 0 to 1.25. The boost in efficiency is because the slurry functions as a cementation material that occupies the location of heating cases when taken out at the end of the heating process, filling the cracks and voids caused by the heating process and covering the parts of treated soils.
- At a 15% settlement ratio, the magnitude of the ultimate bearing capacity ratios reduces from 14.3 to 11.4 for models 1.25 to 1.75 (W/C).
- At a settlement ratio of 15%, the values of the bearing ratio ( $q_u/C_u$ ) for the 3, 14, and 28 days of the heating processes with cement grouting at a water-cement ratio of 1.25 have emerged as 71.70, 88.19, and 98, respectively.

#### Author contributions

Conceptualization, A. Shareeh, M. AL- Neami, and F. Rahil; writing—original draft preparation, A. Shareeh, M. AL-Neami, and F. Rahil; writing—review and editing, A. Shareeh, M. AL- Neami, and F. Rahil; supervision, M. AL- Neami, and F. Rahil. All authors have read and agreed to the published version of the manuscript.

#### Funding

This research received no specific grant from any funding agency in the public, commercial, or not-for-profit sectors.

#### Data availability statement

The data that support the findings of this study are available on request from the corresponding author.

#### Conflicts of interest

The authors declare that there is no conflict of interest.

#### References

- [1] N. M. Tarsh, M. A. Al-Neami, and K. Y. H. Al-Soudany, Variation of Consistency Limits and Compaction Characteristics of Clayey Soil with Nanomaterials, *J. Eng. Technol.*, 39 (2021) 1257–1264. <https://doi.org/10.30684/etj.v39i8.1930>
- [2] M. A. M. Al-Neami, Reducing settlement of soft soils using local materials, *J. Eng. Technol.*, 28 (2010) 6649–6661. <https://doi.org/10.30684/etj.28.23.4>
- [3] M. M. Abu-Zreig, N. M. Al-Akhras, and M. F. Attom, “Influence of heat treatment on the behavior of clayey soils, *Appl. Clay Sci.*, 20 (2001) 129–135. [https://doi.org/10.1016/S0169-1317\(01\)00066-7](https://doi.org/10.1016/S0169-1317(01)00066-7)
- [4] M. A. M. Al-Neami., F. H .Raheel, & Y. H. Al-Ani, Behavior of Cohesive Soil Reinforced by Polypropylene Fiber, *J. Eng. Technol.*, 38 (2020) 801–812. <http://dx.doi.org/10.30684/etj.v38i6A.109>
- [5] M. Y.Fattah, M. M. Al-Ani, & M. T. A Al-Lamy, Studying collapse potential of gypseous soil treated by grouting, *Soils Found.*, 54 (2014) 396–404. <https://doi.org/10.1016/j.sandf.2014.04.008>
- [6] M. N. Ibragimov, Characteristics of Soil Grouting by Hydro-Jet Technology, *Soil Mech. Found. Eng.*, 50 (2013) 200-205. <https://doi.org/10.1007/s11204-013-9234-8>
- [7] A. H.Shareef, M. A. Al-Neami, & F. H. Rahil, Some of The Field and Laboratory Studies on Grouting Properties for Weak Soils: A Review. *Int. J. Intell. Syst. Appl. Eng.*, 11 (2023) 131–141.
- [8] H. Duan, Z. Jiang, S. Zhu, P. Yao, and Q. Sun, “New composite grouting materials: Modified urea–formaldehyde resin with cement, *Int. J. Min. Sci. Technol.*, 22 (2012) 195–200. <https://doi.org/10.1016/j.ijmst.2011.08.009>
- [9] L. Faramarzi, A. Rasti, and S. M. Abtahi, “An experimental study of the effect of cement and chemical grouting on the improvement of the mechanical and hydraulic properties of alluvial formations, *Constr. Build. Mater.*, 126 (2016) 32–43. <https://doi.org/10.1016/j.conbuildmat.2016.09.006>

- [10] A. Varol and S. Dalgıç, "Grouting applications in the Istanbul metro, Turkey. Tunnelling Underground Space Technol., 21 (2006) 602–612. <https://doi.org/10.1016/j.tust.2005.11.002>.
- [11] M. El Tani, Grouting rock fractures with cement grout, Rock Mechanics and Rock Engineering, 45 (2012) 547–561. <http://dx.doi.org/10.1007/s00603-012-0235-0>
- [12] J. Funehag and G. Gustafson, Design of grouting with silica sol in hard rock–New methods for calculation of penetration length, Part I. Tunnelling Underground Space Technol., 23 (2008) 1–8. <https://doi.org/10.1016/j.tust.2006.12.005>
- [13] Q. S. Liu, C. B. Lu, B. Liu, and X. L. Lu, Research on rheological behavior for cement grout considering temperature and hydration time effects, Chin. J. Rock Mech. Eng, 33 (2014) 3730–3740. <http://dx.doi.org/10.13722/j.cnki.jrme.2014.s2.042>
- [14] Z. Zhong-Miao, Z. O. U. Jian, H. E. Jing-Yi, and W. Hua-qiang, Laboratory tests on compaction grouting and fracture grouting of clay, Chin. J. Geotech. Eng., 31(2009) 1818–1824.
- [15] Q. F. Huang, X. G. Li, X. Guo, and K. Atsushi, "Hydraulic fracture extending during slurry shield tunneling in cohesive soil," Yantu Gongcheng Xuebao/ Chin. J. Geotech. Eng., 32 (2010) 712–717.
- [16] B. M. Das, Principles of geotechnical engineering. Cengage learning, 2021.